

## Direct deposition of inorganic–organic hybrid semiconductors and their template-assisted microstructures

V.K. Dwivedi<sup>a</sup>, J.J. Baumberg<sup>b</sup>, G. Vijaya Prakash<sup>a,\*</sup>

<sup>a</sup>Nanophotonics Lab, Department of Physics, Indian Institute of Technology Delhi, Hauz Khas, New Delhi 110016, India

<sup>b</sup>Nanophotonics Centre, Cavendish Laboratory, University of Cambridge, Cambridge CB30HE, UK

### HIGHLIGHTS

- ▶ New fabrication methodology for self-organized inorganic–organic hybrids.
- ▶ Strongly confined exciton emission and photoconductive properties.
- ▶ Simple bottom-up fabrication for device applications.

### ARTICLE INFO

#### Article history:

Received 28 May 2012

Received in revised form

19 August 2012

Accepted 25 October 2012

#### Keywords:

Quantum wells

Microstructure

Photoluminescence spectroscopy

Crystal structure

Electrochemical techniques

### ABSTRACT

A straight-forward method is developed to deposit a new class of self-organized inorganic–organic (IO) hybrid,  $(C_{12}H_{25}NH_3)_2PbI_4$ . These IO hybrid structures are stacked-up as natural multiple quantum well structures and exhibit strong room-temperature exciton emission and other multifunctional features. Here it is successfully demonstrated that these materials can be directly carved into 2D photonic structures from the inexpensive template-assisted electrochemical deposition followed by solution processing. The applicability of this method for many such varieties of IO-hybrids is also explored. By appropriately controlling the deposition conditions and the self-assembly templates, target structures are developed for new-generation low-cost photonic devices.

© 2012 Elsevier B.V. All rights reserved.

### 1. Introduction

Recent progress in the field of multifunctional inorganic–organic (IO) hybrids has generated new possibilities for optoelectronic devices such as thin film transistors, solar cells, photodetectors and light emitting diodes (LEDs), etc [1–3]. Physical and optical properties are distinctly dominated by the favorable combination of their inorganic and organic counterparts. One of the IO hybrid families, in the form of  $(R-NH_3)_2MX_4$  (where R is organic moiety, M is a metal ( $Pb^{2+}$ ,  $Sn^{2+}$ , etc.) and X is halogen ( $I^-$ ,  $Br^-$ ,  $Cl^-$ , etc.)), are stacked low-dimensional layers of organic and inorganic moieties to form multiple quantum-well structures (IO-MQWs). In these structures, ‘quantum wells’ of the 2D inorganic semiconducting layers are clad by ‘barriers’ of the wider bandgap organic layers. Due to large dielectric mismatch (giving dielectric confinement) combined with the quantum confinement, these

hybrids show stable excitons with large binding energy giving rise to highly intense room-temperature absorption and emission resonances [4–18]. Based on the complexity of self-assembly, structural complexity of inorganic network and organic conformation within the layers of inorganic matrix, fabrication methods are generally from conventional chemical synthesis routes [5–7]. Various alternatives were also demonstrated in the recent past in view of using these IO-hybrids directly into device fabrication. These are dual-source fabrication [19], Langmuir–Blodgett (LB) film production [20], single source thermal ablation [21], layer-by-layer deposition [22], spray pyrolysis [23], low-temperature melt processing [24] and one-step intercalation process [4]. Patterning into nano/microstructures using techniques, such as direct writing and other lithographic techniques, were also explored [25,26]. In general, for device fabrication a much simpler and direct fabrication from low-cost and easy methods is essential.

Wavelength-ordering of host material (into 1D, 2D and 3D) and then incorporating emitting low-dimensional guests is the basis of a new class of research. In these new photonic composites, the electron-photon interaction either completely modifies or

\* Corresponding author. +91 11 2659 1326; fax: +91 11 2658 1114.

E-mail address: [prakash@physics.iitd.ac.in](mailto:prakash@physics.iitd.ac.in) (G.V. Prakash).

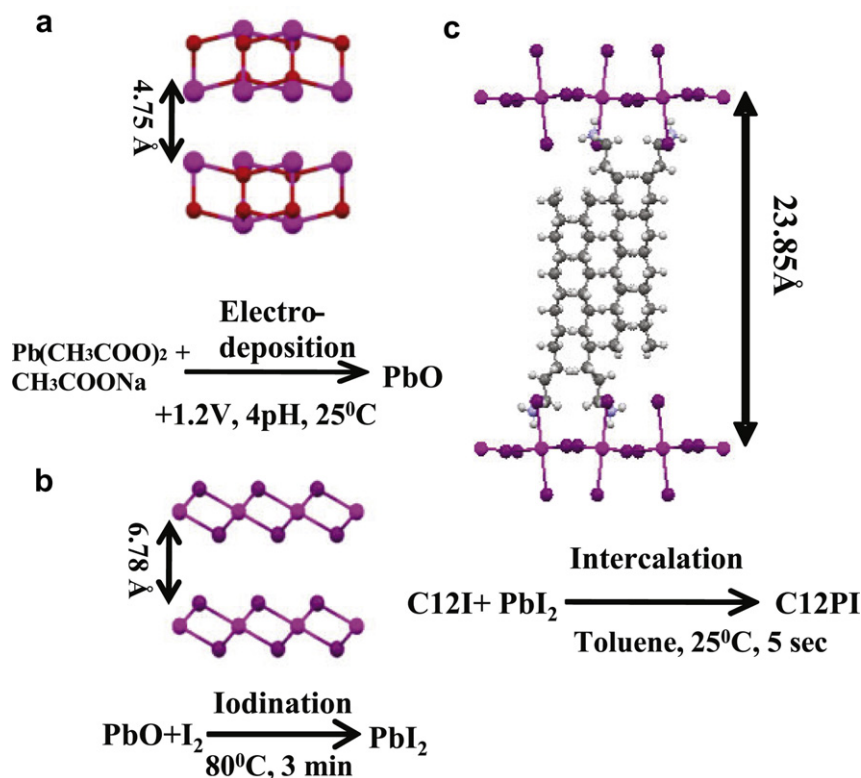


Fig. 1. Schematic representation of fabrication process steps and crystal structure packing of PbO, PbI<sub>2</sub> and C12PI.

enhances the emitting nature of the guest material [27–30]. Usual fabrication is based on expensive and complex top-down approaches; involving direct deposition of materials followed by patterning. One of the inexpensive alternative approaches for 2D and 3D passive photonic structures is a template-assisted bottom-up method. This method is based on natural self-assembled templates and subsequent casting into the interstitial spaces of these templates by reduction of materials through precipitation or electrochemical deposition [31,32]. Electrochemical deposition, usually for highly conducting materials, is a technique that ensures complete filling of interstitial spaces with high-density materials. Recently the ability of this technology to create various photonic structures from inorganic semiconductors (such as CdSe, ZnO) was successfully demonstrated for a wide range of device applications [31–36]. However, obtaining quality semiconductors, either inorganic or organic or hybrids, from electrochemical deposition technique has always been a formidable task due to low conductivity issues.

Here we demonstrate, for the first time, the ability to fabricate strongly emitting IO-hybrids directly from much simpler and inexpensive electrochemical deposition techniques followed by solution processing. These hybrid films show strong room-temperature exciton-related absorption and photoluminescence as well as strong photoconductive characteristics. Further it is also demonstrated that these highly emitting materials can be directly carved into 2D micro structures using self-assembly template-assisted growth. Having optimized deposition conditions, it is thus possible to fabricate these highly emitting materials into 2D and 3D wavelength-scale ordered photonic structures for a wide range of optoelectronic device applications.

## 2. Experiment

Here the demonstration for one of the IO hybrids from the (R-NH<sub>3</sub>)<sub>2</sub>MX<sub>4</sub> family, (C<sub>12</sub>H<sub>25</sub>NH<sub>3</sub>)<sub>2</sub>PbI<sub>4</sub> (decadodecyl ammonium

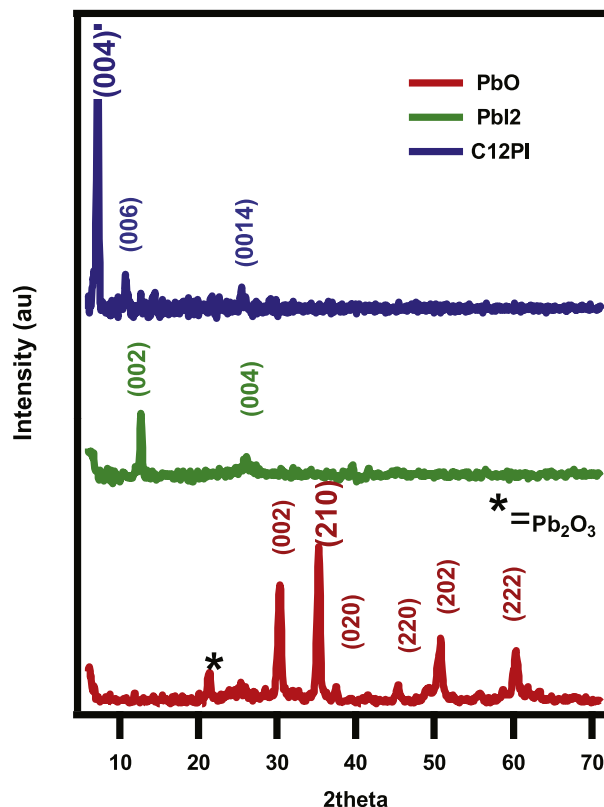
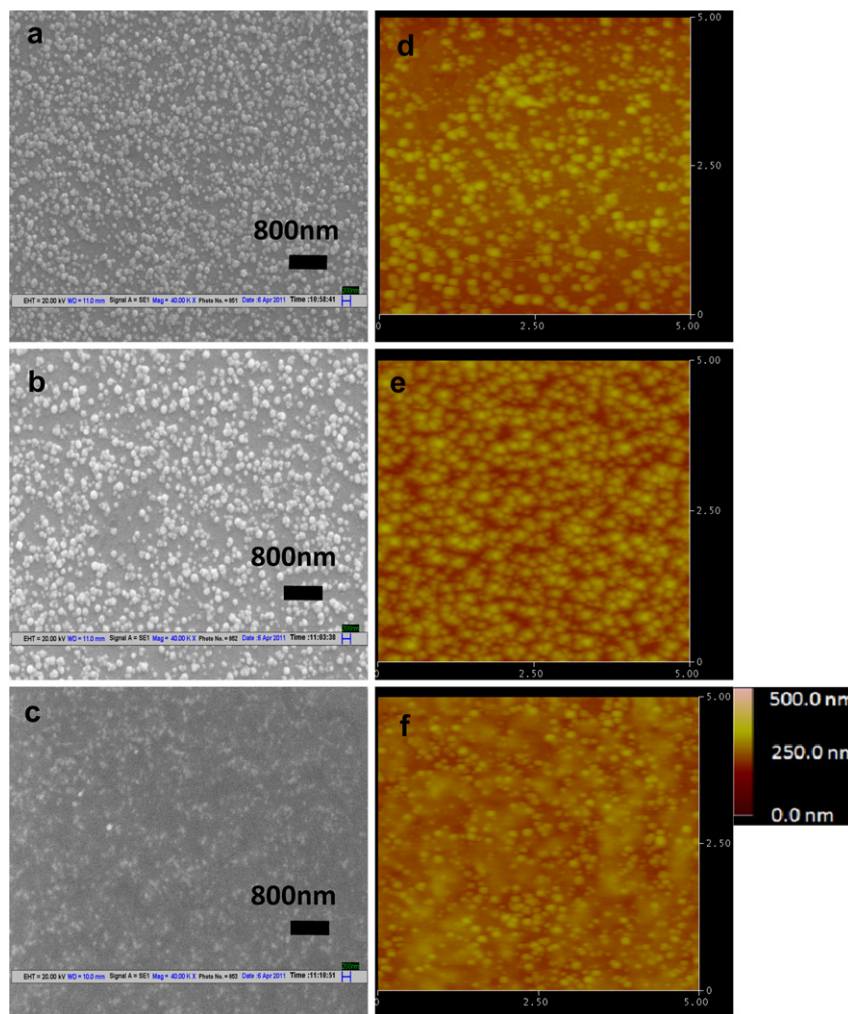


Fig. 2. X-ray diffraction patterns of PbO, PbI<sub>2</sub> and C12PI thin films.



**Fig. 3.** SEM images of (a) PbO, (b) PbI<sub>2</sub>, and (c) C12PI thin films processed from three-step method. AFM pictures of respective films of PbO, PbI<sub>2</sub> and C12PI are shown as figures (d), (e) and (f), respectively.

lead (II) iodide, hereafter C12PI) thin film fabrication is explained. The fabrication follows three steps. (i) First PbO thin films are electrochemically deposited, (ii) then conversion of PbO into PbI<sub>2</sub> proceeds and finally (iii) conversion of PbI<sub>2</sub> into desired IO hybrid is achieved through an intercalation process. Electrochemical deposition is from a three-electrode method using platinum mesh as the counter electrode and saturated calomel electrode (SCE) as reference electrode. Electrochemical deposition of PbO is carried out with the aqueous solutions of acetates 0.1 M Pb(CH<sub>3</sub>COO)<sub>2</sub> and 0.1 M CH<sub>3</sub>COONa at pH 4.0 onto conducting ITO glass substrates [37,38]. During the potentiostatic deposition, a potential of 1.2 V vs. SCE at room-temperature is used to obtain desired PbO thin films. Thickness of the film is optimized by controlling the deposition parameters such as time, deposition potential, etc. The resultant film thickness was measured by AFM and thickness profilometer. Later, these PbO thin films are exposed to iodine vapors in an enclosed dark glass chamber under controlled temperature to convert PbO into PbI<sub>2</sub>. Time of iodination, temperature, humidity and partial pressure are appropriately controlled during this process [39]. For typical iodination of 100 nm thick PbO into PbI<sub>2</sub> film, exposure time of 3 min at constant temperature of 80 °C is used. Finally these PbI<sub>2</sub> films are converted into desired C12PI films using the recently developed intercalation method [4]. Essentially this method involves intercalation of organic moieties into the empty spaces of layered PbI<sub>2</sub>. Here the intercalation process critically depends on

organic moiety sizes, solvent concentration, temperature and intercalation time. In this experiment, the pre-synthesized organic moiety C<sub>12</sub>H<sub>25</sub>NH<sub>3</sub>I (hereafter C12I) is dissolved in toluene (40 mg in 5 ml) and PbI<sub>2</sub> films are directly exposed to C12I solutions. Here it is ensured that the choice of solvent and intercalation time does not affect the surface morphology of PbI<sub>2</sub> as well as the resultant C12PI films. Typical intercalation times of 5 s at room-temperature are used in the present case. We have satisfactorily verified this method using other organic moieties (such as CHI [4,29]) as well. Fig. 1 schematically represents the crystal structure packing, viewed along the c-axis for individual entities PbO, PbI<sub>2</sub> and C12PI and their layer separation. Crystal structure information has been obtained from available single crystal XRD data [12,40,41]. Fig. 1 also represents the fabrication process steps and chemical recipes.

To demonstrate template-assisted growth [31,32], polymer sphere (of 3 μm diameter) templates are prepared by a sedimentation method in which polymer microspheres self-assemble (hexagonal type) onto a pre-defined area (~1 cm<sup>2</sup>) of ITO glass substrate. Desired PbO (110 nm thickness) are electrodeposited into the interstitial spaces of self-assembled polymer spheres. Subsequently, the polymer spheres were removed using appropriate organic solvents, resulting in PbO inverted voids as the perfect replica of the spheres. These PbO microstructures are then converted into PbI<sub>2</sub> and later into C12PI using the methods explained earlier.

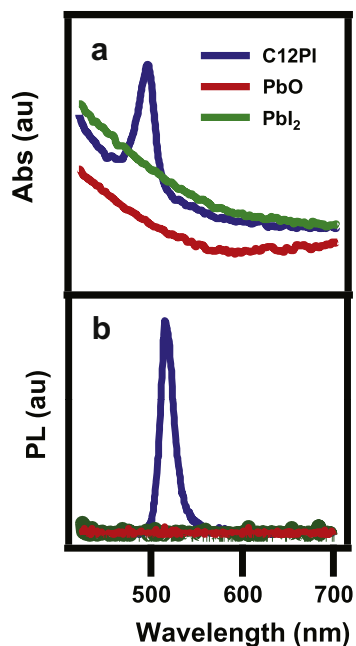


Fig. 4. Room-temperature (a) absorption and (b) photoluminescence spectra of PbO, Pbl<sub>2</sub> and C12PI thin films.

Techniques including Glancing Angle X-Ray Diffraction (GA-XRD), confocal microscopy, Scanning Electron Microscopy (SEM) and Atomic Force Microscopy (AFM) are used to characterize the structural properties. Photoluminescence (PL) and absorption spectra are recorded through a spectrometer using a 410 nm excitation laser for PL and a white-light source for absorption measurements.

### 3. Results and discussion

Inorganic–organic hybrids (C12PI) are two-dimensional layered perovskites, broadly regarded as naturally self-assembled multiple quantum-well (MQW) structures where sheets of extended octahedral [PbI<sub>6</sub>] and organic spacer layers are alternately stacked. However, such self-assembly is complex and the fabrication is through conventional chemical synthesis [5–7] and thin films are usually made from spin-coating techniques. Therefore a simple and direct method, compatible to device fabrication is hereby established. The fabrication follows the conversion of electrodeposited PbO thin films into Pbl<sub>2</sub> and later into desired C12PI, as explained in the experimental section. Firstly smooth and uniform PbO films are achieved by appropriately controlling electrochemical deposition parameters. According to XRD patterns (Fig. 2), the deposited films are predominantly in PbO orthorhombic crystalline phase with a PbO network spacing of 4.78 Å along the *c*-direction. Later, these films are iodinated into Pbl<sub>2</sub> following the process described in Section 2. As evidenced by XRD results (Fig. 2), the electrodeposited PbO is completely converted into Pbl<sub>2</sub> after iodination. The crystal structure (Fig. 1) of Pbl<sub>2</sub> contains edge-sharing layered PbI<sub>3</sub> extended networks [4] along the *c*-axis, therefore the XRD patterns (Fig. 2) are dominated by (001)(*l* = 2,4) crystal planes with an interplanar separation, *d* = 6.78 Å. Finally, these completely converted Pbl<sub>2</sub> thin films are used to intercalate with pre-synthesized organic iodide (C12I) to obtain the desired C12PI thin films. Strong diffraction of (001) (*l* = 4,6,14) planes in XRD patterns (Fig. 2) confirm the layered arrangement and the substantial exfoliation of layers of parent Pbl<sub>2</sub> due to intercalation of organic moiety. The estimated layer-to-layer exfoliation is from *d* = 6.78 Å to 23.84 Å when Pbl<sub>2</sub> is converted into C12PI. As reported previously, C12PI crystallizes in the orthorhombic space group of Pbc<sub>a</sub> in which the asymmetric unit consists of half a (PbI<sub>4</sub>)<sup>2-</sup> anion and one (C<sub>12</sub>H<sub>25</sub>NH<sub>3</sub>)<sup>+</sup> cation [6,12]. Here, well-ordered organic and inorganic layers (with thicknesses ~6 Å and ~10 Å, respectively) are stacked-up alternately along the *c*-direction with layers infinitely

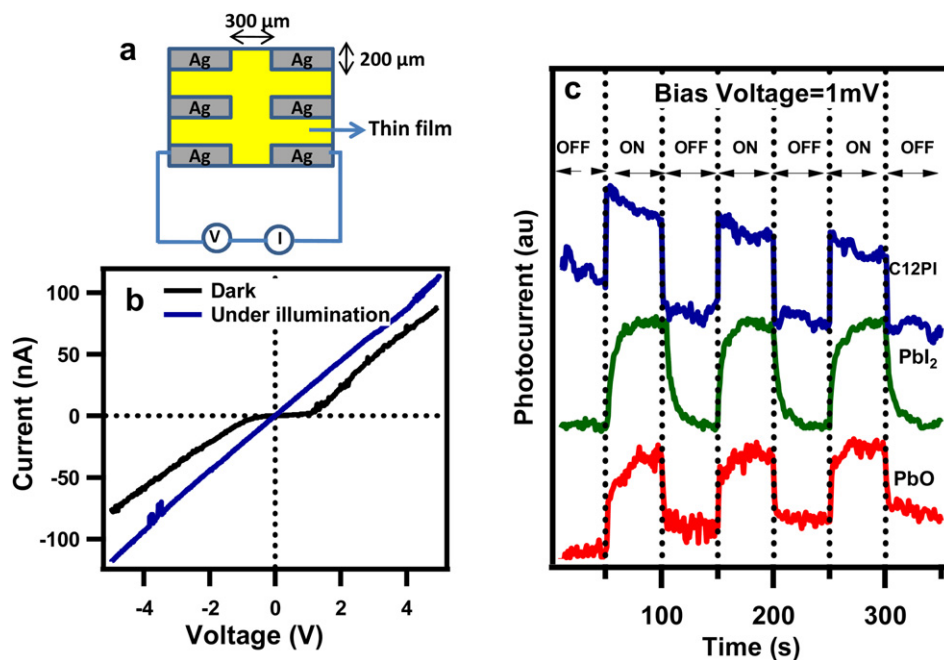
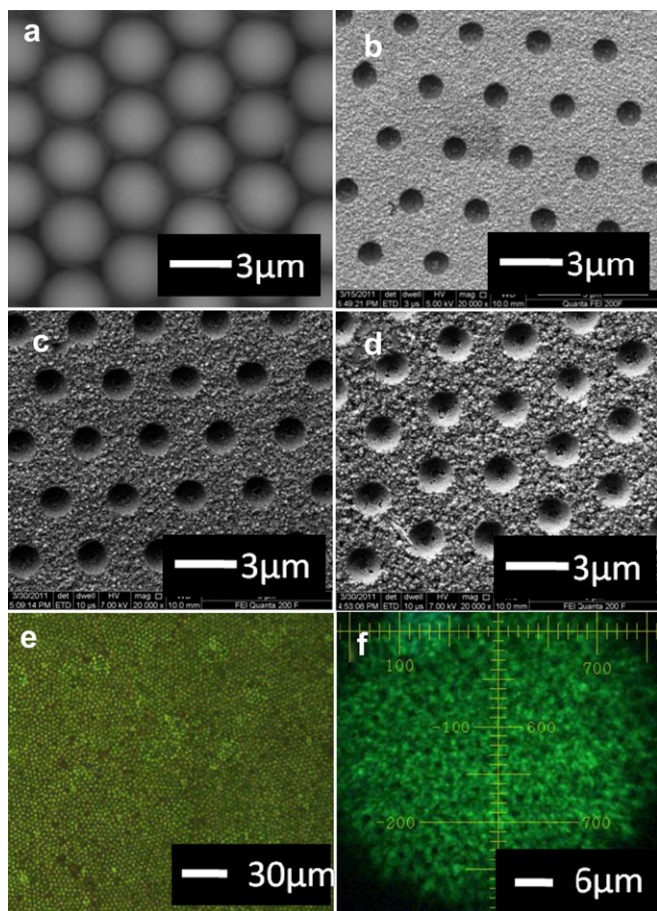


Fig. 5. (a) Schematic metal contacts for photocurrent response measurements. (b) The current–voltage plots for dark and illumination conditions for C12PI thin film. (c) Photocurrent ON–OFF characteristics of PbO, Pbl<sub>2</sub> and C12PI thin films (under applied bias voltage of 1 mV). For PbO and C12PI the response is recorded with 410 nm illumination whereas for Pbl<sub>2</sub> it is 532 nm (see text).



**Fig. 6.** SEM images of (a) self-assembled sphere templates, template-assisted grown (b) PbO, (c) PbI<sub>2</sub> and (d) C12PI microstructures. Microscope (e) dark-field and (f) photoluminescence ( $\lambda_{\text{ex}} = 410 \text{ nm}$ ) high-resolution images of C12PI microstructures.

extended in the *ab* plane [5,6,29]. We have also satisfactorily verified applicability of this method using other organic moieties (such as C<sub>6</sub>H<sub>9</sub>C<sub>2</sub>H<sub>4</sub>NH<sub>3</sub>I (known as CHI)) and other inorganic hosts (such as SnI<sub>2</sub>) and those results will be discussed elsewhere.

Since the conversion of electrodeposited PbO into C12PI is through a chemical process, it is essential to understand the effect of the process on the surface morphology. In order to show the surface quality of obtained thin films, SEM and AFM studies are performed. Fig. 3a–c shows the SEM images of obtained PbO, PbI<sub>2</sub> and C12PI thin films. The surface roughness extracted from AFM scans (Fig. 3d–f) for PbO, PbI<sub>2</sub> and C12PI films (25, 23 and 18 nm, respectively) demonstrates  $\lambda/20$  surface quality before and after chemical processing. Such improved surface quality from electrodeposited and chemically processed thin films is desirable for device-oriented structures.

To exemplify the multifunctional ability for low-cost large area optoelectronic devices, photoluminescence and photocurrent response of these morphological controlled PbO, PbI<sub>2</sub>, and C12PI thin films are also demonstrated. Photoluminescence and absorption of the obtained films are recorded at room temperature and are shown in Fig. 4. While PbO and PbI<sub>2</sub> do not show any resonant results, thin film of C12PI shows strong and narrow absorption and emission peaks at 490 nm and 510 nm, respectively. Due to low-dimensionality and large dielectric mismatch, stable room-temperature excitons are formed within the inorganic network with large binding energies [4–7]. Therefore the observed strong and narrow exciton absorption and emission peaks (typically FWHM  $\sim 20 \text{ nm}$ ) are attributed to the room temperature excitons,

confined within a PbI network of C12PI. The estimated optical bandgaps from absorption spectra (2.10 eV, 2.53 eV and 2.70 eV for PbO, PbI<sub>2</sub> and C12PI respectively) are also in close agreement with the reported values [5,39,42,43].

Photocurrent experiments were carried out by applying a bias voltage between thermally evaporated silver contacts on top of the film (schematic contacts are shown in Fig. 5a). These silver contact patterns have width of 200  $\mu\text{m}$  with 300  $\mu\text{m}$  spacing between the contacts. The area between the contacts is exposed by unfocused low-power ( $\sim 5 \text{ mW}$ ) 410 nm and 532 nm CW lasers and photocurrent results are obtained under various applied bias voltages. Fig. 5b represents typical current–voltage (*I*–*V*) curves for C12PI thin films in the dark and illuminated conditions. These illumination wavelengths are above and below bandgap of these materials, respectively. While the measurement conditions are the same for all three thin films, PbO and C12PI films show considerable photocurrent response only for the above bandgap illumination (410 nm laser light), whereas PbI<sub>2</sub> does not show any appreciable results for the light of this wavelength. However, strong photocurrent response is observed in PbI<sub>2</sub> films for the 532 nm illumination which is much below the estimated optical bandgap (2.52 eV). Fig. 5c shows the ON–OFF photocurrent characteristics of PbO, C12PI (under 410 nm illumination) and PbI<sub>2</sub> (under 532 nm illumination). The photoresponse of PbI<sub>2</sub>, as evidenced by ON–OFF exposure, is comparatively slower than PbO and C12PI (Fig. 5c). Such relatively slow below-bandgap photoresponse in PbI<sub>2</sub> is possibly due to defect related levels present near to the conduction band [44,45]. In PbO, the photocurrent is likely to be governed by absorbed oxygen that captures an electron with a small probability for recombination and also increases the holes life times [42,46]. By contrast in C12PI, the photocurrent is basically from band-to-band transitions within the exfoliated extended network of PbI<sub>3</sub> sheets present in these natural quantum well structures. While the carriers are generated within the bands, recombination dynamics possibly involve confined excitons as well. Therefore, the generation and recombination mechanisms of photocarriers in such IO-hybrids could of special interest for further exploration with respect to the quantum/dielectric confinement effects and exciton dissociation processes. While these results are of preliminary nature, they broadly suggest that the photoresponse in C12PI is significantly enhanced, with enhanced photocurrent speed and efficiency than the parent materials PbO and PbI<sub>2</sub> [47–49].

After having optimized conditions, we investigated approaches to fabricate 2D and 3D periodic and quasi-periodic nano/microstructures from template-assisted growth techniques [31,32]. Here we demonstrate micron-scale 2D periodic highly emitting IO hybrid (C12PI) structures, using template-assisted electrochemical growth. This method can be easily extended to wavelength scale and even for nano-scaled structures. Firstly, uniform electrochemical filling of PbO into interstitial spaces of close-packed sphere templates has been done from electrochemical deposition, using the deposition parameters discussed previously. The microstructures obtained, after removal of the template, are processed to obtain PbI<sub>2</sub> and later C12PI. Fig. 6 shows SEM images of obtained microstructured PbO, PbI<sub>2</sub> and C12PI thin films. The thickness of film was fixed at 110 nm and the resulted void diameter is of 1  $\mu\text{m}$ . Such thickness optimization is required since recently it is demonstrated that this type of IO-hybrids are sensitive to thickness induced stacking imperfections, which directly results in the rapid change in their exciton-related emission/absorption behavior [6,29]. The thickness-dependent disorder produces uneven crystalline planes, and as a consequence, a shift in the exciton PL peak and/or broad defect emission is observed [6,29]. As seen from microscopic and photoluminescence images, these structures are uniform over large scales and are highly luminescent with controlled roughness below

20 nm. The void diameter of electrodeposited PbO microstructure is about 1.1  $\mu\text{m}$  and after iodination ( $\text{PbI}_2$ ) and intercalation (C12PI) the diameters are 1.5 and 1.6  $\mu\text{m}$ , respectively. However, the periodicity (3  $\mu\text{m}$ ) remains the same even after conversion of PbO into  $\text{PbI}_2$  and C12PI. Such void dimension change is expected due to the crystal structure packing readjustment during conversion of PbO into  $\text{PbI}_2$  and C12PI. Furthermore, during the process of obtaining C12PI, organic moiety (C12I) intercalation exfoliates the  $\text{PbI}_2$  film significantly due to the increase in the *c*-axis spacing. However, such thickness enhancement and crystal structure packing variation might possibly be compensated by the volume readjustment of constituents within the interstitial 3D structure, which preserve the dimensions. It is to be noted that fabrication of such three-dimensionally defined structures from infiltration methods, using conventionally synthesized IO-hybrids is impossible since the resultant films obtained from slow solvent evaporation preferentially forms into flakes resembling single crystalline morphology [6]. From these experiments, the fabrication of 2D and 3D structures with lateral templates below 500 nm is also clearly possible and such experiments are under progress. These structures promisingly indicate new directions to large area devices, such as LEDs and photovoltaic devices. Our techniques can be further expanded in different ways, for example electrodepositing such highly emitting IO-hybrids onto metal micro/nano structures to explore new applications in plasmonic photonics [50].

#### 4. Conclusion

Here we demonstrate, for the first time, a simple three-step approach to fabricate high-quality and highly luminescent inorganic–organic self-assembled hybrid structures. By appropriately controlling the fabrication conditions, such highly luminescent lead (II) based IO hybrids can be molded into desired micro/nano scaled devices for potential utilization in optoelectronic applications. These new classes of photonic hybrids, fabricated from inexpensive approaches, show promising multifunctional optoelectronic properties.

#### Acknowledgments

This work is part of UK-India Education Research Initiative (UKIERI) and High-impact research initiative (IIT Delhi) and also part funded by EPSRC grants EP/H027130/1 and EP/G060649/1. The technical help rendered by project assistant, Mr. Deep Punj is appreciated. VKD acknowledges UGC, India for senior research fellowship.

#### References

- [1] S. Ren, L.Y. Chang, S.K. Lim, J. Zhao, M. Smith, N. Zhao, V. Bulovi, M. Bawendi, S. Gradecak, *Nano Lett.* 11 (2011) 3998–4002.
- [2] C. Sanchez, B. Julian, P. Belleville, M. Popall, *J. Mater. Chem.* 15 (2005) 3559–3592.
- [3] C. Sanchez, C.B. Lebeau, F. Chaput, J.P. Boilot, *Adv. Mater.* 15 (2003) 1969–1994.
- [4] K. Pradeesh, J.J. Baumberg, G. Vijaya Prakash, *Appl. Phys. Lett.* 95 (2009) 033309.
- [5] (a) K. Pradeesh, J.J. Baumberg, G. Vijaya Prakash, *Appl. Phys. Lett.* 95 (2009) 173305;
- (b) K. Pradeesh, J.J. Baumberg, G. Vijaya Prakash, *J. Appl. Phys.* 111 (2011) 013511.
- [6] G. Vijaya Prakash, K. Pradeesh, R. Ratnani, K. Saraswat, M.E. Light, J.J. Baumberg, *J. Phys. D: Appl. Phys.* 42 (2009) 185405.
- [7] K. Pradeesh, M. Agarwal, K.K. Rao, G. Vijaya Prakash, *Solid State Sci.* 12 (2010) 95–98.
- [8] Z. Cheng, J. Lin, *Cryst. Eng. Commun.* 12 (2010) 2646–2662.
- [9] V.V. Naik, S. Vasudevan, *J. Phys. Chem. C* 114 (2010) 4536–4543.
- [10] S. Barman, N.V. Venkataraman, S. Vasudevan, R. Seshadri, *J. Phys. Chem. B* 107 (2003) 1875–1883.
- [11] K. Gauthron, J.S. Lauret, L. Doyennette, G. Lanty, A. Al. Choueiry, S.J. Zhang, A. Brehier, L. Largeau, O. Mauguin, J. Bloch, E. Deleporte, *Opt. Express* 18 (2010) 5912–5919.
- [12] D.G. Billing, A. Lemmerer, *New J. Chem.* 32 (2008) 1736–1746.
- [13] S. Zhang, G. Lanty, J.S. Lauret, E. Deleporte, P. Audebert, L. Galmiche, *Acta Mater.* 57 (2009) 3301–3309.
- [14] K. Chondroudis, D.B. Mitzi, *Chem. Mater.* 11 (1999) 3028–3030.
- [15] Z.Y. Cheng, Z. Wang, R.B. Xing, Y.C. Han, J. Lin, *Chem. Phys. Lett.* 376 (2003) 481–486.
- [16] M. Era, S. Morimoto, T. Tsutsui, S. Saito, *Appl. Phys. Lett.* 65 (1994) 676–678.
- [17] H. Abid, A. Samet, T. Dammak, A. Mlayah, E.K. Hlil, Y. Abid, *J. Lumin.* 131 (2011) 1753–1757.
- [18] I. Koutselas, P. Bampoulis, E. Maratou, T. Evagelinou, G. Pagona, G.C. Papavassiliou, *J. Phys. Chem. C* 115 (2011) 8475–8483.
- [19] T. Matsushima, K. Fujita, T. Tsutsui, *Jpn. J. Appl. Phys.* 43 (2004) 11999–12001.
- [20] K. Ikegami, *J. Chem. Phys.* 121 (2004) 2337–2347.
- [21] D.B. Mitzi, M.T. Prikas, K. Chondroudis, *Chem. Mater.* 11 (1999) 542–544.
- [22] Z.Y. Cheng, H.F. Wang, Z.W. Quan, C.K. Lin, J. Lin, Y.C. Han, *J. Cryst. Growth* 285 (2005) 352–357.
- [23] T. Matsui, A. Yamaguchi, Y. Takeoka, M. Rikukawa, K. Sanui, *Chem. Commun. (Cambridge)* 3 (2002) 1094.
- [24] D.B. Mitzi, D.R. Medeiros, P.W. DeHaven, *Chem. Mater.* 14 (2002) 2839–2841.
- [25] J.D. Torrey, S.E. Vasko, A. Kapetanovic, Z. Zhu, A. Scholl, M. Rolandi, *Adv. Mater.* 22 (2010) 4639–4642.
- [26] H.J. Jeon, K.H. Kim, Y.K. Baek, D.W. Kim, H.T. Jung, *Nano Lett.* 10 (2010) 3604–3610.
- [27] V.K. Dwivedi, K. Pradeesh, G. Vijaya Prakash, *Appl. Surf. Sci.* 257 (2011) 3468–3472.
- [28] V. Bulovi, V.B. Khalfin, G. Gu, P.E. Burrows, S.R. Forrest, *Phys. Rev. B* 58 (1998) 3730–3740.
- [29] K. Pradeesh, J.J. Baumberg, G. Vijaya Prakash, *Opt. Express* 17 (2009) 22171–22178.
- [30] S. Noda, M. Fujita, T. Asano, *Nat. Photon* 1 (2007) 449–458.
- [31] G. Vijaya Prakash, R. Singh, A. Kumar, R.K. Mishra, *Mater. Lett.* 60 (2006) 1744–1747.
- [32] G. Vijaya Prakash, K. Pradeesh, A. Kumar, R. Kumar, S.V. Rao, M.L. Markham, J.J. Baumberg, *Mater. Lett.* 62 (2008) 1183–1186.
- [33] M.A. McLachlan, H. Rahman, B. Illy, D.W. McComb, M.P. Ryan, *Mater. Chem. Phys.* 129 (2011) 343–348.
- [34] P.N. Bartlett, T. Dunford, M.A. Ghanem, *J. Mater. Chem.* 12 (2002) 3130–3135.
- [35] M.A. Ghanem, P.N. Bartlett, P. De Groot, A. Zhukov, *Electrochem. Commun.* 6 (2004) 447–453.
- [36] M.C. Tsai, D.X. Zhuang, P.Y. Chen, *Electrochim. Acta* 55 (2010) 1019–1027.
- [37] S. Sawatani, S. Ogawa, T. Yoshida, H. Minoura, *Adv. Funct. Mater.* 15 (2005) 297–302.
- [38] I. Zhitomirsky, L. Galor, A. Kohn, H.W. Henniske, *J. Mater. Sci. Lett.* 14 (1995) 807–810.
- [39] T.K. Chaudhuri, H.N. Acharya, *Mat. Res. Bull.* 17 (1982) 279–286.
- [40] R.J. Hill, *Acta Crystallogr. C* 41 (1985) 1281–1284.
- [41] P. Terpstra, H.G.K. Westenbrink, *Proc. K. Ned. Akad. Wet B* 29 (1926) 431.
- [42] J. Schottmiller, *J. Appl. Phys.* 37 (1966) 3505–3510.
- [43] E.A. Maljarov, S.G. Tikhodeev, N.A. Gippius, *Phys. Rev B* 51 (1995) 14370–14378.
- [44] G.D. Currie, J. Mudar, O. Risgin, *Appl. Optics* 6 (1967) 1137–1138.
- [45] A.E. Dugan, H.K. Hknisch, *Phys. Rev.* 171 (1968) 1047–1051.
- [46] L. Heijne, *J. Phys. Chem. Solids* 22 (1961) 207–212.
- [47] Y. Kawabata, M.Y. Fujita, Y. Takeoka, M. Rikukawa, *Synth. Met.* 159 (2009) 776–779.
- [48] X. Hong, T. Ishihara, A.V. Nurmikko, *Solid State Commun.* 84 (1992) 657–661.
- [49] G.C. Papavassiliou, G.A. Mousdis, I.B. Koutselas, *Int. J. Mod. Phys. B* 15 (2001) 3727–3731.
- [50] G. Vijaya Prakash, M. Kaczmarek, A. Dyadyusha, J.J. Baumberg, G. D'Alessandro, *Opt. Express* 13 (2005) 2201–2209.